JOURNAL OF SOLID STATE CHEMISTRY 137, 295–301 (1998)
ARTICLE NO. SC977739

Structural and Surface Acid/Base Properties of Hydrotalcite-Derived MgAlO Oxides Calcined at Varying Temperatures

Jianyi Shen,*,[1] Mai Tu,* and Chen Hu†

*Department of Chemistry and †National Laboratory of Solid State Microstructures, Nanjing University, Nanjing 210093, China

Received August 20, 1997; in revised form December 15, 1997; accepted December 18, 1997

This paper describes the influence of calcination temperature on bulk and surface properties of MgAlO binary oxide derived from the hydrotalcite precursor. MAS ^{27}Al NMR revealed that significant phase transitions occurred in the samples calcined at 673, 873, and 1073 K. These transitions seem to be important in determining the surface acid/base properties of the samples. Microcalorimetric adsorptions of NH_3 and CO_2 showed that the acidity of these samples decreases in the order: γ-Al_2O_3 > 673 K > 873 K ≈ 1073 K, while the basicity follows the order: MgO > 873 K > 1073 K > 673 K. IR spectroscopy revealed that the surface acid/base sites of the calcined hydrotalcite samples are mainly Lewis type. © 1998 Academic Press

INTRODUCTION

Hydrotalcite-like compounds consist of brucite-like layers containing octahedrally coordinated bivalent (*e.g.*, Mg^{2+}, Ni^{2+}, Zn^{2+}, Cu^{2+}) and trivalent (*e.g.*, Al^{3+}, Fe^{3+}) cations, as well as interlayer anions (*e.g.*, CO_3^{2-}, NO_3^-, Cl^-, OH^-) and water. These compounds have been used as precursors of catalysts and catalyst supports (1–14). For example, calcined Mg–Al hydrotalcites promote a variety of base-catalyzed reactions, such as aldol condensations and polymerization reactions (2, 3, 13). Recently, we found that Pt–Sn catalysts supported by calcined Mg–Al hydrotalcite were effective for the dehydrogenation of butane and were more selective and resistant to deactivation than their conventional alumina-supported counterparts (14).

The surface acid/base properties of hydrotalcite-derived MgAlO oxides with Mg/Al molar ratios ranging from 3 to 12 have been studied by using microcalorimetry and infrared spectroscopy (1). The MgAlO oxides calcined at 773 K exhibited moderate acidity and basicity between MgO and Al_2O_3; their surface acid/base sites were mainly Lewis type. The effect of calcination temperature on the strengths of acid/base sites on these materials as measured by microcalorimetric adsorption has not been reported so far.

In this work, we studied physical properties such as surface area, pore volume, bulk phase, and coordination state of Al^{3+} cations, as well as the surface acidity/basicity of calcined Mg–Al hydrotalcite vs calcination temperature. These physical properties were characterized using N_2 adsorption at liquid N_2 temperature, X-ray diffraction (XRD), and magic-angel-spinning ^{27}Al nuclear magnetic resonance (MAS ^{27}Al NMR). The surface acid/base properties were determined by adsorptive microcalorimetry (15–17) and infrared spectroscopy (IR) (18, 19), employing NH_3 and CO_2 as the probe molecules.

EXPERIMENTAL

The hydrotalcite with Mg/Al molar ratio of 3 was prepared following the method described in Ref. (1). Specifically, two aqueous solutions containing $(NH_4)_2CO_3$ and NH_4OH, and $Al(NO_3)_3$ and $Mg(NO_3)_2$ were added dropwise and alternately in 30 min, into about 250 ml deionized water at room temperature. The precipitate was washed with distilled water and dried at 393 K overnight. Then it was converted into MgAlO binary oxides by calcination (heating rate: 10 K min^{-1}) for 6 h in air at 673, 873, and 1073 K. $Mg(OH)_2$ was precipitated by adding NH_4OH solution to $Mg(NO_3)_2$ solution at room temperature, followed by washing and drying. MgO was then obtained by calcining the $Mg(OH)_2$ at 673 K for 6 h. A commerical γ-Al_2O_3 was used as the reference in this work.

XRD was performed on a Shimadzu XD-3A X-ray diffractometer using Cu$K\alpha$ radiation at a scan rate of 4° min^{-1}. Surface area and pore size were measured by N_2 adsorption at 77 K on a Micromeritics ASAP 2000 apparatus using the BET and BJH methods. Before the measurements, the samples were usually evacuated at 573 K to pressures lower than 4×10^{-3} Torr.

MAS ^{27}Al NMR spectra were recorded with a Bruker MSL-300 spectrometer operating at a frequency of 78.17 MHz (magnetic field of 7 T) with sample spinning rate

[1] To whom correspondence should be addressed. Fax: 0086-25-3317761. E-mail: jyshen@netra.nju.edu.cn.

0022-4596/98 $25.00

of 3.8 kHz. The chemical shifts were measured relative to a 1 M aqueous solution of $Al(NO_3)_3$.

Microcalorimetric adsorptions of NH_3 and CO_2 were carried out at 423 K using a Tian-Calvet heat-flow microcalorimeter. The details of the apparatus and the experimental conditions can be found elsewhere (15). Before the measurements, the samples were calcined *in situ* again for 4 h followed by evacuation for 2 h at 673 K.

Infrared spectra were collected at 4 cm^{-1} resolution with a Bruker IFS66V FT-IR system. The self-supported wafer of each sample with approximately 20 mg cm^{-2} was treated in the same manner as the microcalorimetric sample. Probe molecules of NH_3 or CO_2 were dosed onto the sample at 423 K for 0.5 h. Then the sample was cooled to 293 K. The IR data were collected after evacuating the sample at 293 and 423 K.

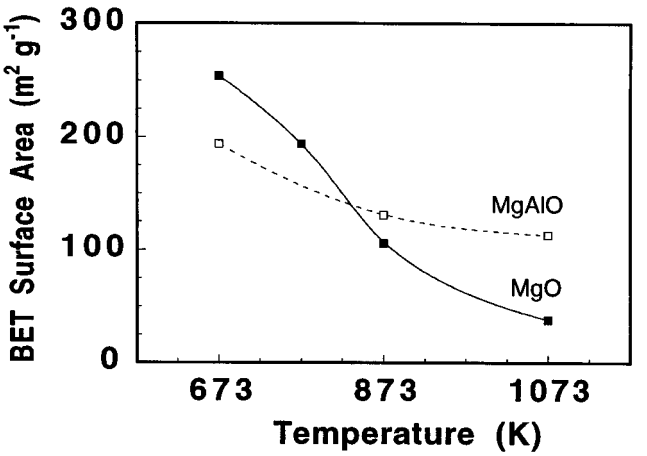

FIG. 1. Surface area vs calcination temperature for the MgO and MgAlO samples.

RESULTS AND DISCUSSION

Figure 1 shows the plots of BET surface area vs calcination temperature for the MgAlO and MgO samples. With the increase of calcination temperature, the surface area of the MgAlO sample decreases from 194 to 115 m^2 g^{-1}, while that of MgO decreases from 254 to 38 m^2 g^{-1}. Apparently, the MgAlO binary oxides are more stable under heat treatment than MgO, in agreement with the results reported in the literature (2, 5). Figure 2 shows the pore size distribution of the MgAlO samples calcined at various temperatures. These pore size distribution curves were obtained from the desorption branches of the corresponding hysteresis loops. It is seen that most pores are populated around 18 nm for these samples. However, the volume of smaller pores decreases with the increase of calcination temperature, resulting in an increase of average pore size as listed in Table 1. Table 1 summarizes some physical properties of the MgAlO oxides and those of MgO for comparison.

XRD patterns of the calcined hydrotalcite samples are shown in Fig. 3. Only the pattern characteristic of the MgO phase can be seen in the sample calcined at 673 K. This result indicates that Al^{3+} cations are highly dispersed in the structure of MgO without the formation of spinel species. Calcination of the hydrotalcite at 873 and 1073 K resulted in relatively intensive diffraction lines of MgO, owing to the increased particle size and/or improved crystallinity in the samples. In addition, the spinel phase, $MgAl_2O_4$, appeared in the sample calcined at 873 K, and this phase became more intense for the sample calcined at 1073 K.

NMR can probe structure on a smaller scale than XRD. It is more sensitive to phase transitions and less affected by particle size and degree of crystallinity of samples (20–29). Thus, MAS ^{27}Al NMR was performed in this work to probe the environment changes of Al^{3+} cations that were difficult to characterize by XRD. It is known that all the Al^{3+} occupy the octahedral sites in hydrotalcite before calcination (4, 27) and that the calcination may yield phases with spinel-like structure in which Mg^{2+} and Al^{3+} occupy octahedral and tetrahedral sites in the close-packed layers of O^{2-} anions (2). The NMR spectra collected for the calcined hydrotalcite samples are shown in Fig. 4. It is seen that the ^{27}Al resonances of the MgAlO samples fall into two distinct regions around 80 and 12 ppm, corresponding to Al^{3+} in tetrahedral (Al_T) and octahedral (Al_O) sites, respectively (20–23). The octahedral and tetrahedral distributions of Al^{3+} can be estimated by integrating the areas under the corresponding peaks. The results indicate that the ratio of Al_O/Al_T in the MgAlO samples decreases with the order: 60/40 (673 K) > 55/45 (873 K) > 50/50 (1073 K). Apparently, a transition of Al^{3+} from octahedral to tetrahedral sites occurs upon calcination at the elevated temperatures.

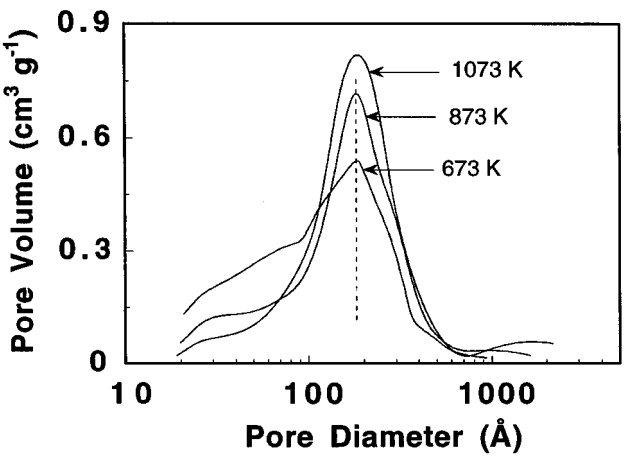

FIG. 2. Distribution of pore size of the MgAlO samples calcined at varying temperatures.

TABLE 1
Physical Properties of Calcined Hydrotalcite Samples and MgO

	MgAlO				MgO	
Calci. temp	XRD phase	BET area ($m^2\ g^{-1}$)	Av. pore diam. (nm)	Pore vol. ($cm^3\ g^{-1}$)	Av. pore diam. (nm)	Pore vol. ($cm^3\ g^{-1}$)
673 K	MgO	195	9.2	0.43	9.6	0.42
873 K	MgO, spinel	132	13	0.41	18	0.35
1073 K	MgO, spinel	114	17	0.45	17	0.16

Because of the formation of spinel phase in the samples calcined at 873 and 1073 K, the site distribution of cations in the $MgAl_2O_4$ spinel as revealed by MAS NMR should be considered here. In fact, the $MgAl_2O_4$ spinel has been studied extensively using the MAS NMR (24–27). In particular, Mackenzie *et al.* studied the thermal decomposition of Mg–Al hydrotalcite and phase variations of MgAlO binary oxide at temperatures from 473 to 1473 K (27) by XRD and NMR. All of these studies observed the migration of cations in the spinel lattice upon heat treatment, usually the migration of Al^{3+} from octahedral to tetrahedral sites, consistent with our findings in this work. In the unit cell of $MgAl_2O_4$ spinel, there are 32 oxygens and 24 cations with 8 cations tetrahedrally coordinated and 16 octahedrally coordinated. This kind of spinel can be expressed as $(A_{1-i}B_i)[A_iB_{2-i}]O_4$, where A and B denote bivalent and trivalent cations, respectively, and parentheses and brackets denote tetrahedral and octahedral sites, respectively. The two extreme forms of the spinel are normal and inverse when i equals 0 and 1 respectively. But i can also be any number between 0 and 1, which expresses the degree of inversion and can be evaluated according to the ratio of octahedral to tetrahedral sites occupied by B cations. In our case, the value of i was calculated to be 0.8, 0.9, and 1 for the samples calcined at 673, 873 and 1073 K, respectively. Thus, an inverse spinel structure seems to have been formed for our sample calcined at 1073 K. However, these values are much higher than those reported in the literature for the $MgAl_2O_4$ spinel (24–27), probably due to the different states of the samples. In fact, our samples were mixtures of MgO and the spinel when calcined at 873 and 1073 K, while the samples studied in the references (24–26) were pure and were usually prepared by solid reaction at temperatures higher than 1473 K. However, Mackenzie *et al.* also found that the fraction of tetrahedral Al^{3+} was about 0.5 when the Mg–Al hydrotalcite was calcined at 673 K. Unfortunately, no correlation can be made at present between XRD and NMR

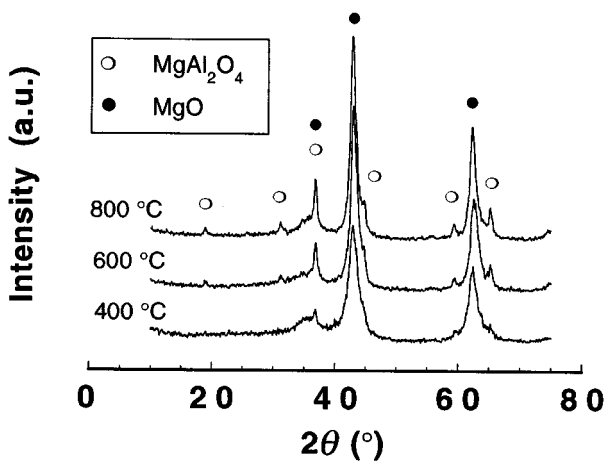

FIG. 3. XRD patterns of the MgAlO samples calcined at varying temperatures.

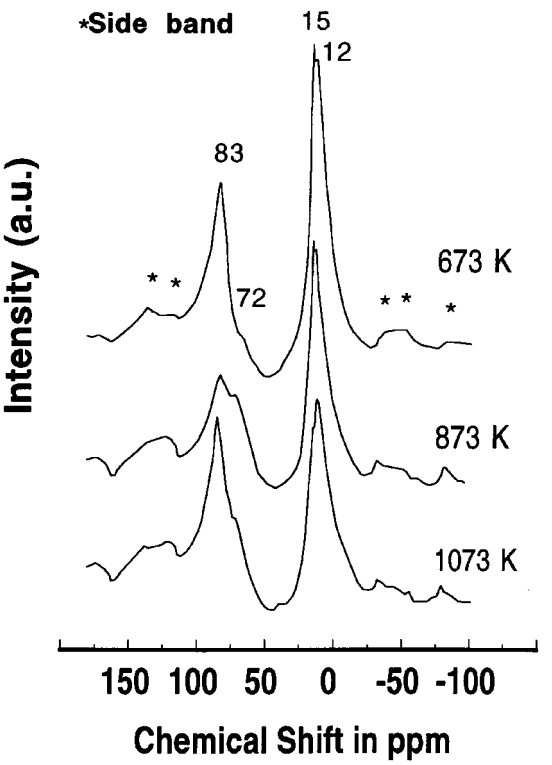

FIG. 4. MAS ^{27}Al NMR spectra of the MgAlO samples calcined at varying temperatures.

results, since the XRD cannot provide information about the site distributions. In this regard, NMR may be a more informative tool than XRD, since the former provided the information that can be related to the surface acid/base properties that will be discussed later in this paper.

Actually, more subtle influences on the coordination surroundings of Al^{3+} are reflected by the spread of chemical-shift values. The ^{27}Al chemical shift is known to be sensitive to the second nearest-neighbor coordination sphere (20–22). For binary compounds, the chemical shift becomes more positive with the smaller electronegativity of elements bonded to Al–O polyhedra (28, 29). For the spectra in Fig. 4, each band from an octahedral or tetrahedral site splits into two peaks, indicating that both sites have two distinct coordination states. The peak with the chemical shift at 12 ppm can be assigned to Al_O bonded to Mg^{2+} (Al_O–O–Mg). The peak at 15 ppm is very sharp, which is indicative of a well defined, crystalline, octahedral phase. Shen *et al.* (1) observed a similar peak at 16 ppm and pointed out that the nature of this phase was not apparent, but that it was not characteristic of the oxides since the quantity of this phase might be less than 1%. Two peaks (83 and 72 ppm) can be clearly observed in the tetrahedral band. The Al_T resulting in the 83 ppm peak evidently has higher electron density and thereby can be assigned to Al_T–O bonded to Mg^{2+}(Al_T–O–Mg), while the 72 ppm peak can be assigned at Al_T–O bonded to Al^{3+}(Al_T–O–Al). Therefore, upon calcination at elevated temperatures, several phase transitions may take place. Apparently, a transition from Al_O–O–Mg (12 ppm) to Al_T–O–Mg (83 ppm) occurs when the sample is calcined at 673 K. This transition continues when the sample is calcined at 873 and 1073 K, since the ratio of Al_O/Al_T continues to decrease with the increase of calcination temperature. In addition, another transition from Al_T–O–Mg (83 ppm) to Al_T–O–Al (72 ppm) might occur when the sample is calcined at 873 K. However, this latter transition seems to be reversed, *i.e.*, a transition from Al_T–O–Al (72 ppm) back to Al_T–O–Mg (83 ppm) might take place, when the sample is calcined at 1073 K. Thus, the sample calcined at 873 K seems to be in a transition state that may exhibit different acid/base properties, which will be presented below.

Figures 5 and 6 show the plots of the differential heat vs coverage for CO_2 and NH_3 adsorptions, respectively, on the samples calcined at the different temperatures. Apparently, the Mg–Al binary oxides exhibit lower basicity than MgO and lower acidity than γ-Al_2O_3, consistent with the results reported previously (1). However, the difference of acid/base properties of these binary oxides displayed is also apparent. The basicity of the samples can be arranged in the order: MgO > 873 K > 1073 K > 673 K, while the order for the acidity is: γ-Al_2O_3 > 673 K > 873 K $\approx$ 1073 K.

Figure 5 clearly shows that the sample calcined at 873 K displays significantly higher basicity than those calcined at

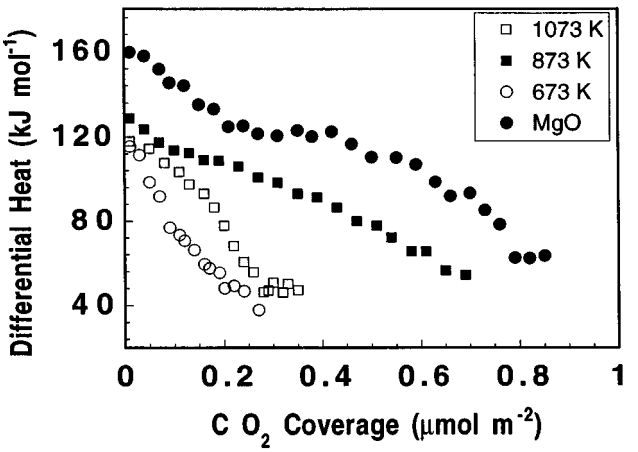

FIG. 5. Differential heat vs coverage for CO_2 adsorption on the MgO and MgAlO samples calcined at varying temperatures.

673 and 1073 K in terms of both the initial differential heat and the saturation coverage for the CO_2 adsorption. This sample exhibits a large peak at 72 ppm in its NMR spectrum (Fig. 4). The peak is attributable to the structure Al_T–O–Al, *i.e.*, the Al_T–O tetrahedrons with other Al^{3+} cations as the nearest neighbours, which might be converted from the structure Al_T–O–Mg, *i.e.*, the Al_T–O tetrahedrons with Mg^{2+} cations as the nearest neighbors. The migration of Al_T away from adjacent Mg^{2+} may leave more O^{2-} anions surrounding the Mg^{2+}. In fact, the IR results to be presented shortly show that the stronger base sites are associated with those O^{2-} anions having Mg^{2+} as the nearest neighbors. In addition, quantum calculations reveal that the main factor that influences the generation of stronger basicity is an increase in O^{2-} anions coordinated to the Mg^{2+} near to the central O^{2-} in the base site (30). Thus, it may be concluded that the sample calcined at 873 K in the transition state may possess sites having relatively more O^{2-} anions coordinated to Mg^{2+} explaining the sample's enhanced basicity.

Figure 6 shows that the sample calcined at 673 K displays stronger acidity than those calcined at 873 and 1073 K. This sample has the higher Al_O/Al_T ratio (60/40) as determined by ^{27}Al NMR. McKenzie *et al.* (7) proposed based on NMR and XPS (X-ray photoelectron spectroscopy) that the calcined hydrotalcites underwent enrichment of Al_T on the surface. In addition, the McKenzie group showed that the surface Al_T exhibited poor activity for the conversion of 2-propanol to propene, which is a typical acid-catalyzed reaction. Our XPS results indicated that no surface enrichment of Al^{3+} occurred in our samples calcined at the various temperatures. Therefore, we may attribute the acidity of the sample calcined at 673 K to the octahedrally coordinated Al^{3+} on the surface. In fact, this sample calcined at a relatively low temperature may have more defects that allow more accessible Al^{3+} cations to adsorb NH_3.

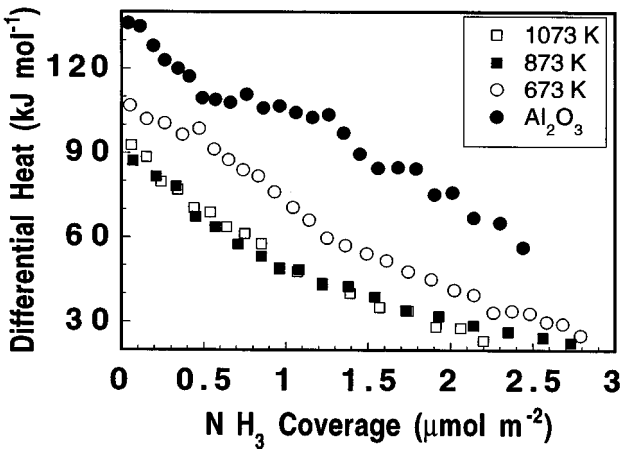

FIG. 6. Differential heat vs coverage for NH_3 adsorption on the γ-Al_2O_3 and MgAlO samples calcined at varying temperatures.

The FT–IR spectra of CO_2 adsorption on the calcined hydrotalcite samples are shown in Fig. 7. These spectra are similar to each other, with six bands at around 1650, 1570, 1390, 1270, 1230, and 1070 cm^{-1}, indicating that the calcination temperature has little influence on the nature of surface base sites. After evacuation at 423 K, three bands at around 1570, 1390, and 1270 cm^{-1} remain; the bands 1570 and 1390 cm^{-1} can be assigned to unidentate species and the band 1270 cm^{-1} to bidentate, carbonate species associated with Mg^{2+} cations (31, 32). Evacuation at 423 K leads to the disappearance of the bands at around 1650, 1230, and 1070 cm^{-1}, indicating that the corresponding species are formed on weaker base sites. The bands at 1650 and 1230 cm^{-1} can be assigned to bidenatate carbonate species associated with Al^{3+} cations (30). It is thus clear that the O^{2-} anions associated with Al^{3+} cations exhibit weaker basicity than those associated with Mg^{2+} cations.

The FT–IR spectra collected after NH_3 adsorption at 423 K are shown in Fig. 8. The spectrum for γ-Al_2O_3 is similar to that reported previously (1). The bands at 1623 and 1238 cm^{-1} are due to NH_3 adsorbed on Lewis acid sites (Al^{3+}), while the bands at 1690, 1486, and 1391 cm^{-1} belong to NH_4^+ species formed between NH_3 and Brønsted acid sites (33). All the calcined hydrotalcite samples exhibit primarily Lewis acidity with the bands at around 1623 and 1180 cm^{-1}. The bands in the region between 1300 and 1480 cm^{-1} are hardly seen in the spectra for the calcined hydrotalcite samples due to adsorption of NH_3 on Brønsted acid sites, in agreement with the results reported by Lercher

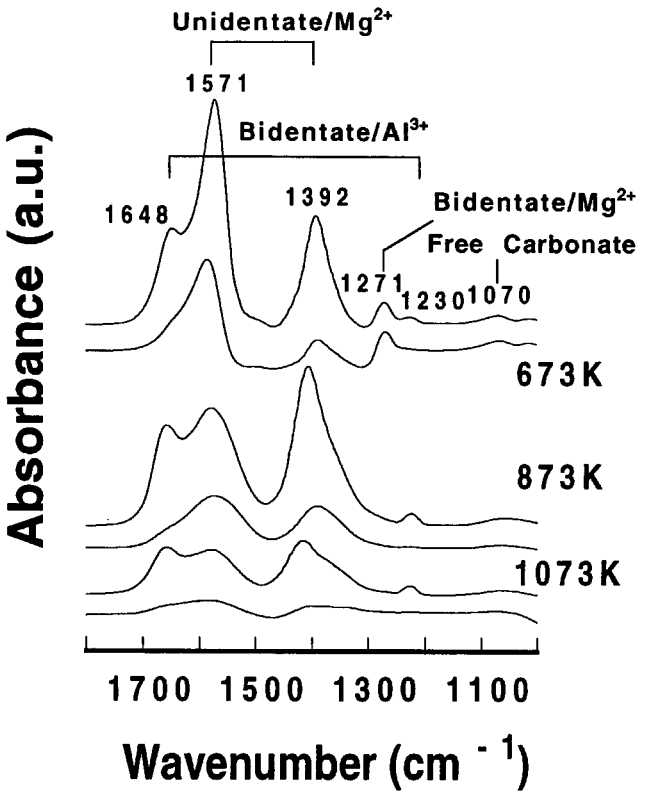

FIG. 7. Infrared spectra for CO_2 adsorption on the MgAlO samples calcined at varying temperatures.

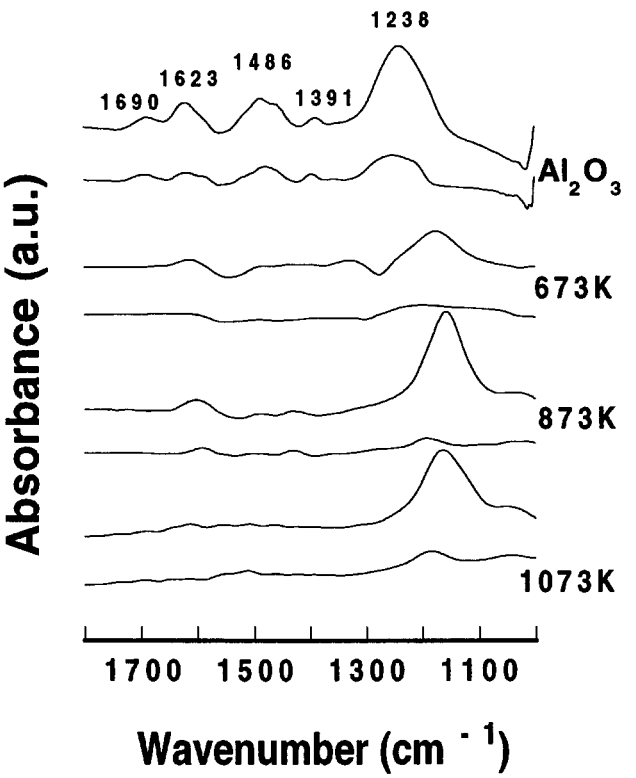

FIG. 8. Infrared spectra for NH_3 adsorption on the γ-Al_2O_3 and MgAlO samples calcined at varying temperatures.

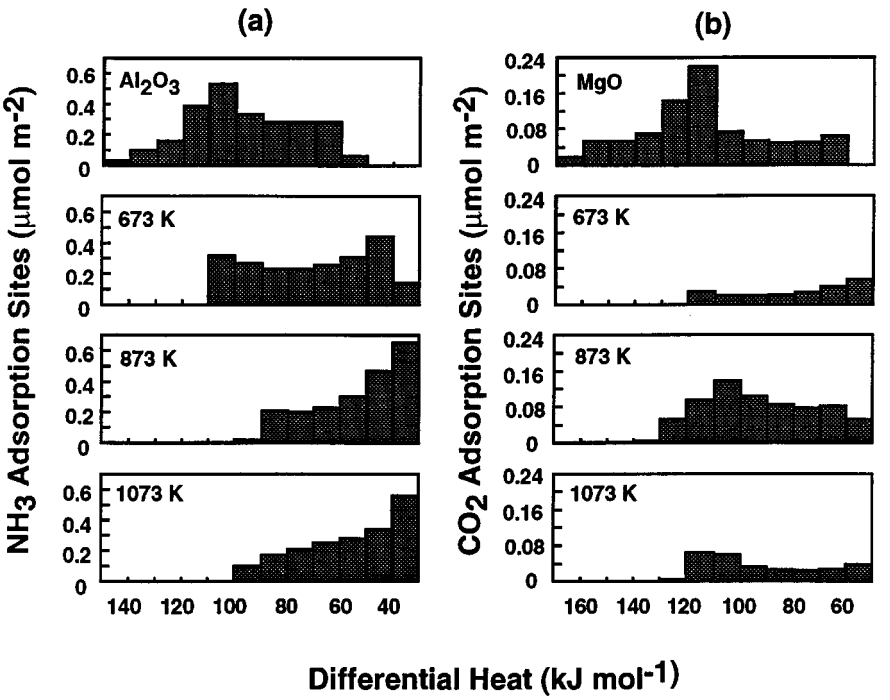

FIG. 9 . Histograms of the distribution of interaction strengths for (a) NH_3 and (b) CO_2 adsorption on the γ-Al_2O_3, MgO, and MgAlO samples calcined at varying temperatures.

et al., who found that only Lewis acid sites existed on the mixed oxide MgO–Al_2O_3 (34). After evacuation at 423 K, all the peaks almost disappear, indicating that these sites are not strong for the adsorption of NH_3.

Figure 9 presents a better view of the acid/base strength distributions on the samples. These histograms were generated by first fitting the curves of differential heat vs coverage by polynomials and then using the fitted polynomials to determine the number of adsorbates interacting with surface sites with a differential heat within a given range. As shown in Figure 9a, the sample caclined at 673 K exhibits acidity, with about 0.3 μmol m^{-2} NH_3 adsorption sites between 100 and 110 kJ mol^{-1}, which are not available for the samples calcined at 873 and 1073 K. On the other hand, Figure 9b shows that the sample calcined at 873 K possesses base sites stronger than 120 kJ mol^{-1}. In addition, this sample possesses more base sites with the CO_2 adsorption heat between 60 and 120 kJ mol^{-1} than the samples calcined at 673 and 1073 K.

CONCLUSIONS

In this work, we extended our studies to the effects of calcination temperature on the calcined hydrotalcite. This information may be useful for the hydrotalcite-derived MgAlO binary oxides used as acid/base catalysts and catalyst supports. We confirmed that MgAlO exhibited moderate acidity/basicity, even upon calcination at varying temperatures from 673 to 1073 K. We also confirmed that the MgAlO samples are more stable than MgO toward heat treatment in surface area and pore size. In addition, it was found that the material has relatively uniform pore size distribution centered around 18 nm. It was also found that calcination at 873 K produced the MgAlO with stronger basicity than the samples calcined at 673 and 1073 K, while calcination at 673 K produced the MgAlO sample with stronger acidity than the samples calcined at higher temperatures. This behavior provides more treatment parameters to control the surface acidity/basicity of MgAlO according to needs. Finally, we demonstrated by combining the results of MAS ^{27}Al NMR and microcalorimetric adsorption that the transition state, which has relatively more Al_T–O tetrahedra associated with Al^{3+} (the structure Al_T–O–Al) in the sample calcined at 873 K, may possess sites having relatively more O^{2-} anions coordinated to Mg^{2+}, which show enhanced basicity.

ACKNOWLEDGMENTS

We acknowledge the financial support from the Trans-Century Training Program Foundation for the Talents by the State Education Commission of China and the National Natural Science Foundation of China (29673021). We also appreciate professor Jianyi Shen's valuable discussions

with Professor J. A. Dumesic at his lab in the Department of Chemical Engineering, University of Wisconsin at Madison.

REFERENCES

1. Jianyi Shen, J. M. Kobe, Yi Chen, and J. A. Dumesic, *Langmuir* **10,** 3902 (1994).
2. F. Cavani, F. Trifiro, and A. Vaccari, *Catal. Today* **11,** 173 (1991).
3. W. T. Reichle, *J. Catal.* **94,** 547 (1985).
4. W. T. Reichle, *J. Catal.* **101,** 352 (1986).
5. H. Schaper, J. J. Berg-Slot, and W. H. J. Stork, *Appl. Catal.* **54,** 79 (1989).
6. R. J. Davis and E. G. Derouane, *Nature* **349,** 313 (1991).
7. A. L. McKenzie, C. T. Fishel, and R. J. Davis, *J. Catal.* **138,** 547 (1992).
8. A. Corma, and R. M. Martin-Aranda, *Appl. Catal., A* **105,** 271 (1993).
9. E. Narita, P. Kaviratna, and T. J. Pinnavaia, *Chem. Lett.*, 777 (1993).
10. C. T. Fishel and R. J. Davis, *Langmuir* **10,** 159 (1994).
11. J. M. Lopez, A. Dejoz, and M. I. Vazquez, *Appl. Catal., A.* **132,** 41 (1995).
12. Jianyi Shen, Bin Guang, Mai Tu, and Yi Chen, *Catal. Today* **30,** 77 (1996).
13. V. K. Diez, C. R. Apesteguia, and J. I. Di Cosimo, "Proceedings of the 15th North American Meeting on Catalysis," p. 58 (1997).
14. Jianyi Shen, Mai Tu, and Yi Chen, "Proceedings of the 15th North American Meeting on Catalysis," p. 129 (1997).
15. N. Cardona-Martinez and J. A. Dumesic, *Adv. Catal.* **38,** 149 (1992).
16. A. Auroux and A. Gervasini, *J. Phys. Chem.* **94,** 6371 (1990).
17. Mai Tu, Jianyi Shen, and Yi Chen, *J. Solid State Chem.* **128,** 73 (1997).
18. J. A. Lercher, C. Grundling, and G. Eder-Mirth, *Catal. Today* **27,** 353 (1996).
19. J. C. Lavalley, *Catal. Today* **27,** 377 (1996).
20. J. W. Akitt, *Prog. Nucl. Magn. Reson. Spectrosc.* **21,** 1 (1989).
21. D. Muller and W. Gessner, *Chem. Phys. Lett.* **79**(1), 59 (1981).
22. E. Ohtani, F. Taulelle, and C. A. Angell, *Nature* **314,** 78 (1985).
23. C. S. John, N. C. M. Alma, and G. R. Hays, *Appl. Catal.* **6,** 341 (1983).
24. B. J. Wood, R. J. Kirkpatrick, and B. Montez, *Am. Mineral.* **71,** 999 (1986).
25. G. C. Gobbi, R. Christoffersen, M. T. Otten, B. Miner, P. R. Buseck, G. J. Kennedy and C. A. Fyfe, *Chem. Lett.*, 771 (1985).
26. R. L. Millard, R. C. Peterson, and B. K. Hunter, *Am. Mineral.* **77,** 44 (1992).
27. K. J. D. MacKenzie, R. H. Meinhold, B. L. Sherriff, and Z. Xu, *J. Mater. Chem.* **3,** 1263 (1993).
28. E. Lippma, A. Samoson, and M. Kagi, *J. Am. Chem. Soc.* **108,** 1730 (1986).
29. N. S. Kostarenko, V. M. Mastikhin, I. L. Mudrakovskii and V. P. Shmachkova, *React. Kinet. Catal. Lett.* **30**(2), 375 (1986).
30. H. Kawakami and S. Yoshida, *J. Chem. Soc., Faraday Trans. 2* **80,** 921 (1984).
31. N. D. Parkyns, *J. Phys. Chem.* **75,** 526 (1971).
32. G. Busca and V. Lorenzelli, *Mater. Chem.* **7,** 89 (1982).
33. A. A. Tsyganenko, D. V. Pozdnyakov, and V. N. Filimonov, *J. Mol. Struc.* **29,** 299 (1975).
34. J. A. Lercher, *React. Kinet. Catal. Lett.* **20,** 409 (1982).